information services
gwasanaethau gwybodaeth

Catalytic partial oxidation of cyclohexane by bimetallic Ag/Pd nanoparticles on magnesium oxide

Xi Liu,[a,b,⊥] Marco Conte,[a,c,⊥] Qian He,[a,d] David W. Knight,[a] Damien M. Murphy,[a] Stuart H. Taylor,[a] Keith Whiston,[e] Christopher J. Kiely,[d] Graham J. Hutchings,*[a]

Abstract: The liquid phase oxidation of cyclohexane to cyclohexanol and cyclohexanone was investigated by synthesizing and testing an array of heterogeneous catalysts comprising: monometallic Ag/MgO, monometallic Pd/MgO and a set of bimetallic AgPd/MgO catalysts. Interestingly, Ag/MgO was capable of a conversion comparable to current industrial routes of *ca.* 5%, and with a high selectivity (up to 60%) to cyclohexanol, thus making Ag/MgO an attractive system for the synthesis of intermediates for the manufacture of nylon fibres. Furthermore, following the doping of Ag nanoparticles with Pd, the conversion increased up to 10% whilst simultaneously preserving a high selectivity to the alcohol. Scanning transmission electron microscopy and energy dispersive spectroscopy of the catalysts showed a systematic particle size composition variation with the smaller Ag-Pd nanoparticles being statistically richer in Pd. Analysis of the reaction mixture by Electron Paramagnetic Resonance (EPR) spectroscopy coupled with the spin trapping technique showed the presence of large amounts of alkoxy radicals, thus providing insights for a possible reaction mechanism.

Introduction

The catalytic oxidation of hydrocarbons is a research area or great importance both in industry and academia,[1,2] by virtue of the variety of products that can be obtained from this feedstock.[3,4] The use of O_2 or air as oxidants for the partial oxidation of hydrocarbons to alcohols or ketones, gained considerable attention in recent years.[5] This is because aerobic oxidation processes are greener and cheaper from a reagent cost perspective compared to the use of oxygen transfer reagents, which are more expensive and usually lead to undesired by-products.[6] However, the oxidation of hydrocarbons by means of molecular oxygen is a complex process comprising both catalytic oxidation and autoxidation routes,[7] with the latter precluding selective oxidation processes to a specific or desired product. In this context, the aerobic oxidation of cyclohexane to cyclohexanol and cyclohexanone as precursors for the production of nylon fibres is one of the most important and challenging processes in the petrochemical industry. In fact, this reaction is industrially carried out by exploiting autoxidation pathways promoted by Co complexes.[8,9]There is a strong commercial incentive to run such processes at higher conversion in order to reduce the extent of cyclohexane recycle and therefore save steam. However, the conversion of cyclohexane has in practice to be kept low, in the range of 3-8%, to reduce the presence of uncatalysed and unselective free radical reaction pathways, which occur increasingly at higher conversion and give rise to undesired by-products. Low cyclohexane conversion is therefore required to control the process at acceptable selectivities > 80% towards the two major products commercial products cyclohexanol and cyclohexanone. In a previous study, by using Au-Pd nanoalloys supported on MgO,[10] we found that these catalysts were capable of an enhanced conversion for cyclohexane oxidation of > 10% in the absence of organic initiators, while still preserving a high selectivity to cyclohexanol as shown by Au/MgO catalysts.[11] It was noted however that monometallic Au nanoparticles supported on MgO required the presence of a radical initiator such as AIBN or TBHP to show an appreciable catalytic activity. These studies and their context prompted us to consider the use of Ag and Ag-Pd nanoalloys for cyclohexane oxidation. In this paper, we therefore explore the effect of adding Pd to Ag nanoparticles, and although Ag has proved extremely useful for epoxidation reactions of alkenes,[12] to date it has been largely neglected for the direct oxidation of saturated hydrocarbons.

Results and Discussion

Catalytic activities of Ag Pd and Ag-Pd particles supported on MgO

Monometallic Ag and Pd catalysts prepared using a sol-immobilization (SI) protocol[13] were initially tested as a benchmark for investigating the activity of Ag-Pd nanoalloys (Table 1). Pd/MgO was virtually inactive with a conversion of 0.5%, which is similar to that of a blank oxidation test (*i.e.* one in which no catalyst is present). In contrast, Ag/MgO gave a significant conversion of *ca.* 5%, with an excess of alcohol (56% selectivity), together with a low selectivity to adipic acid (*ca.* 7%). These conversion levels and selectivity indicate that Ag/MgO could be a promising catalyst for this reaction.[14] However, the catalytic activity of Ag nanoparticles showed a marked dependence on the catalyst preparation method used. In fact, if a Ag/MgO catalyst was synthesised *via* impregnation (Table 1), a lower conversion of 2.6% was observed. It should be emphasised that both of these Ag/MgO catalysts display a high selectivity to the alcohol (> 55% in each case). However, the product distribution between the two differently synthesised catalysts is quite different, with Ag/MgO prepared by sol-immobilization produced some adipic acid (*ca.* 7%), whereas Ag/MgO prepared by impregnation led to some cyclohexyl hydroperoxide (CHHP) (*ca.* 7%).

[a]   Dr. X. Liu, Dr. M. Conte, Prof. D. W. Knight, Prof. D. M. Murphy, Prof. S. H. Taylor, Prof. G. J. Hutchings*

        Cardiff Catalysis Institute, School of Chemistry, Cardiff University, Cardiff, CF10 3AT (UK)

        E-mail: hutch@cardiff.ac.uk

[b]   Dr. X. Liu
        Syncat@Beijing, Synfuels China Technology Co.,Ltd,

        Beijing, 101407 (China)

[c]   Dr. M. Conte

        Department of Chemistry, Dainton Building, University of Sheffield, Sheffield, S3 7HF (UK)

[d]   Dr. Q. He, Prof. K. J. Kiely

The difference in catalytic activity between these two catalysts is tentatively attributed to the formation of Ag_2O for the impregnated catalyst.[15] On the contrary, the sol immobilized material presented, rather surprisingly, only metallic Ag (see section: Characterization of the Ag/MgO catalysts using electron microscopy). In view of this, Ag_2O and MgO were individually tested (Table 1). Ag_2O showed a conversion of *ca.* 2% and a similar product distribution to that of the blank test, (*i.e.* a large amount of CHHP). In comparison, MgO was highly selective towards the alcohol, but with a conversion equal to the blank test (*ca.* 1%). Furthermore, despite the conversion levels with MgO and Pd/MgO being statistically identical, no CHHP was detected when Pd/MgO was used. This demonstrates that the metal can promote the decomposition of this CHHP species, which is an important intermediate in the oxidation of cyclohexane (see section: Mechanistic insights and CHHP decomposition).

Importantly, this increase in conversion also preserved a product distribution similar to that observed for the monometallic Ag/MgO catalyst obtained *via* sol -immobilization (*i.e.* with an alcohol-to-ketone ratio, A/K, of *ca.* 2 and adipic acid < 10%). In order to confirm this result, reusability tests were carried out (Table 2). Repeated testing up to four consecutive runs did not show any decrease in catalytic activity, nor any changes in selectivity compared to the initial test, thus showing that the AgPd/MgO catalyst is highly stable under the tests conditions. Therefore, we consider these results highly significant for the development of catalyst materials active towards cyclohexane oxidation.

Table 1. Conversion and product distribution for a series of Pd and Ag catalysts supported over MgO for the partial oxidation of cyclohexane. Reaction conditions: T = 140 ºC, P = 3 bar, reaction time: 17 h.

Catalyst	Conversion (%)	Selectivity (%)				
		K[c]	A[d]	CHHP[e]	AA[f]	Total[g]
Pd/MgO[a]	0.5	32	66	0	0	98
Ag/MgO[a]	4.6	31	56	0	7	97
Ag/MgO[b]	2.6	27	55	7	0	90
MgO	1.0	31	67	0	1	98
Ag_2O	1.9	31	38	25	0	94
Blank	1.1	22	40	35	0	97

[a] Catalyst prepared by sol immobilization method. [b] Catalyst prepared by impregnation method. [c] K = ketone, cyclohexanone. [d] A = alcohol, cyclohexanol. [e] CHHP = cyclohexyl hydroperoxide. [f] AA = adipic acid. [g] Total observed selectivity.

These data prompted us to consider the use of supported Ag-Pd nanoalloys prepared using a sol-immobilization protocol to explore the possibility of synergistic effects between Ag and Pd, analogous to that observed for Au-Pd nanoalloys supported over MgO.[10] A molar ratio of 1:1 between these two metals was initially prepared and tested (Table 2). The simultaneous presence of the two metals (retaining the same total metal loading of 1% wt, as used for the monometallic species, so that the total metal-to-substrate ratio is not changed), doubled the conversion up to *ca.* 10%.

Table 2. Catalytic test and reusability test result using a AgPd/MgO catalyst prepared *via* sol immobilization and a Ag:Pd ratio of 1:1 for the partial oxidation of cyclohexane. Reaction conditions: T = 140 ºC, P = 3 bar, reaction time: 17 h.

Catalyst (and run)	Conversion (%)	Selectivity (%)				
		K[a]	A[b]	CHHP[c]	AA[d]	Total[e]
AgPd/MgO (1st)	9.5	26	52	0	10	89
AgPd/MgO (2nd)	10	30	56	0	8	94
AgPd/MgO (3rd)	10	31	57	0	6	94
AgPd/MgO (4th)	9.8	28	57	0	9	95

[a] K = ketone, cyclohexanone. [b] A = alcohol, cyclohexanol. [c] CHHP = cyclohexyl hydroperoxide. [d] AA = adipic acid. [e] Total observed selectivity.

Characterization of the Ag/MgO catalysts using electron microscopy

In an effort to structurally characterise these Ag/MgO catalysts, as well as provide possible explanations for the dependence of the catalytic activity on the preparation method, high angle annular dark field (HAADF) STEM imaging studies were employed (Figure 1). The monometallic Ag/MgO sample prepared *via* sol-immobilization showed supported Ag metal nanoparticles in the 5-10 nm size-range having an f.c.c. crystal structure (Figure 1(d)). Many of these primary colloidal Ag particles were also found to have congregated into larger polycrystalline aggregates about 20-30 nm in size (Figure 1(c)). It is quite remarkable that although this sample had been exposed to air for many months before STEM examination and yet still presented as metallic Ag. We speculate that the stability of the Ag nanoparticles towards low oxidation states might be attributable to the PVA surfactant used in the preparation method[16] - a stability that also reflects in a high catalyst re-usability for sequentially repeated catalytic tests - with high consistency in conversion and selectivity values (Table 2).

By way of contrast, the monometallic Ag/MgO catalyst synthesised by the impregnation route presented a distinct bimodal size distribution of Ag containing particles (Figure 1(a)). The larger particles had diameters in the 20-40 nm range, whereas the smaller population were in the 1-5 nm size range (Figure 1(b)). Interestingly these smaller Ag particles were more raft-like and irregularly shaped in character and exhibited a definite epitaxial cube-on-cube orientation relationship with the underlying MgO support. The reason for the poorer activity of the impregnation Ag/MgO catalyst is not obvious from this nanostructural analysis.
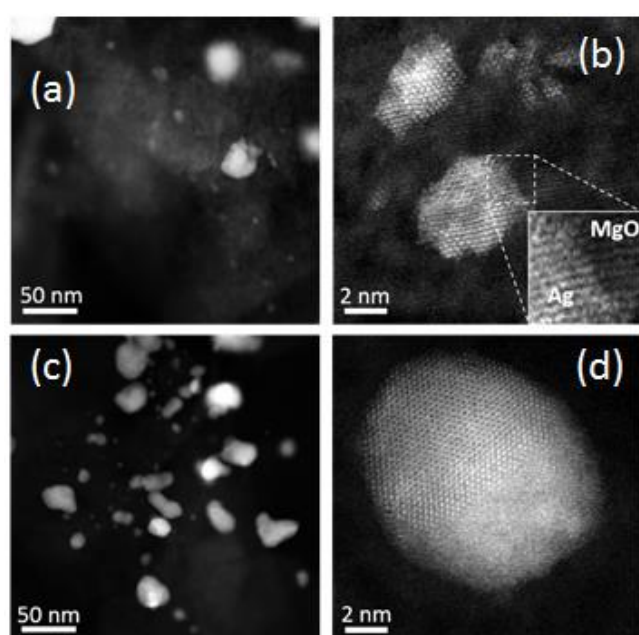
Figure 1. Representative STEM-HAADF images of Ag/MgO catalysts prepared by (a, b) the impregnation method and (c, d) the sol immobilization method. The impregnated Ag catalyst contains (a) relatively large particles about 30 nm in size, as well as (b) smaller raft-like species in the 1-5 nm size range. These smaller species show an epitaxial orientation relationship with the MgO support (inset). The Ag/MgO catalyst prepared *via* sol immobilization appears to have a bi-modal Ag size distribution, containing (c) aggregates of particles about 25 nm in size, and (d) smaller single crystal metallic Ag particles around 5-10 nm in size.

Catalytic activities of AgPd/MgO catalysts with different Ag:Pd molar ratios

In view of these results, and in order to estimate an empirical optimal composition for the bimetallic Ag-Pd/MgO catalyst with the aim of enhancing the conversion for this reaction, a series of catalysts with Pd to Ag molar ratios ranging from 1:10 to 10:1 were prepared *via* sol-immobilization. A detailed description of the product distribution for these materials is reported in Table 3. The highest conversion, in the range of 8-10%, is observed for catalysts having nominal stoichiometries (molar ratio) of Ag_1Pd_3, Ag_1Pd_1, Ag_3Pd_1 and Ag_5Pd_1. However, it should be underlined that Ag and Pd form a continuous solid solution,[17] and to be best of our knowledge no superlattice formation is known for these two elements.

Table 3. Summary of the catalytic activity (conversion and product distribution) of AgPd/MgO catalysts with different Ag:Pd molar ratios for the oxidation of cyclohexane. Reaction conditions: 8.5 g cyclohexane, 3 bar O_2, 6 mg catalysts, 17 hours, 140°C.

Catalyst[a]	Conversion (%)	Selectivity (%)				
		K[b]	A[c]	CHHP[d]	AA[e]	Total[f]
Pd/MgO	0.5	32	66	0	0	98
Ag_1Pd_{10}/MgO	2.3	38	55	0	6	100
Ag_1Pd_5/MgO	3.2	45	46	0	3	94
Ag_1Pd_3/MgO	8	40	45	0	8	93
Ag_1Pd_1/MgO	9.5	26	52	0	10	89
Ag_3Pd_1/MgO	10	27	60	0	8	95
Ag_5Pd_1/MgO	9.3	33	58	0	7	98
$Ag_{10}Pd_1$/MgO	4.6	35	54	0	6	95
Ag/MgO	4.6	31	56	0	7	97

[a] Catalysts prepared by sol immobilization method, with different Ag:Pd molar ratios, as reported by the indexes in subscript next to the metal symbol. [b] K = ketone, cyclohexanone. [c] A = alcohol, cyclohexanol. [d] CHHP = cyclohexyl hydroperoxide. [e] AA = adipic acid. [f] Total observed selectivity.

(a) 50 nm (b) 2 nm MgO Ag (c) 50 nm (d) 2 nm

From these catalytic data the maximum conversion is observed for the compositions: Ag_1Pd_1, Ag_3Pd_1, Ag_5Pd_1, which corresponds to a Ag mole fraction x_{Ag} in between 0.5 and 0.8. In an attempt to rationalize these results, we applied STEM-HAADF imaging together with X-ray energy dispersive spectroscopy (XEDS) analysis to a Ag-Pd/MgO sample prepared *via* the sol-immobilisation route and having a nominal Ag:Pd molar ratio of 1:1. The results revealed a bimetallic catalyst possessing a rather complex structure. In fact, the catalyst was composed of a collection of very large irregularly shaped agglomerates of primary particles, with dimensions of around 30-100 nm (Figure 2(a)), together with a multitude of much smaller isolated particles of 2-5 nm diameter (Figure 2(b)). The composition of these differently sized species were qualitatively analysed by XEDS (Figures 2(c),(d)) It should be noted that a strong overlap between the Pd L peak (2.84 keV) and the Ag L peak (2.98 keV) in this sample precluded any quantatative compositional analysis. However, by comparison with XEDS spectra obtained from monometallic supported Ag and Pd catalyst materials it was possible to deduce the larger nanoparticles were systematically rich in Ag, whereas the population of smaller nanoparticles was always rich in Pd. These observations, combined with the data presented in Table 3, would suggest that the larger particles, which are richer in Ag are probably the most active for the oxidation of cyclohexane.
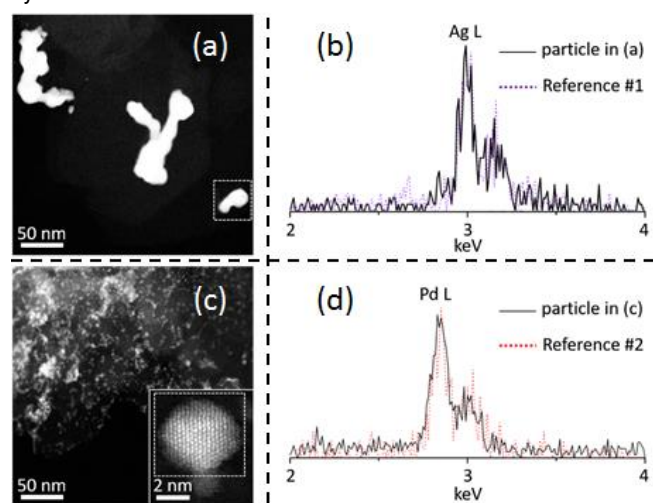

Figure 2. Representative STEM-HAADF images and corresponding XEDS spectra the 1:1Ag-Pd/MgO catalyst prepared by the sol-immobilization method; (a) shows relatively large particles (>50 nm), and the solid line in (b) shows the corresponding XEDS spectrum taken from the highlighted particle in (a). The purple dashed line shows a reference #1 spectrum taken from an Ag particle in the Ag/MgO sol-immobilized catalyst; (c) shows relatively smaller particles. The inset shows a higher magnification image of one such typical metallic Ag-Pd f.c.c. alloy particle viewed along the [110] projection. The solid line in (d) shows the corresponding XEDS spectra taken from the highlighted particle in the inset in (c). The red dashed line shows a reference #2 spectrum taken from a monometallic Pd particle in a suitable reference catalyst, suggesting that these smaller particles are Pd-rich. Both (b) and (d) show that mixing of Ag and Pd components in the alloy samples are rather limited.

The effect of a different Ag:Pd molar ratio impacts only the conversion; there, however, is no obvious trend with molar fraction of Ag for the selectivity in terms of ketone to alcohol molar ratio, K/A ratio, instead. In each case the alcohol is always in excess in the product, and K/A ratio values are, on average (from the amounts of ketone and alcohol in table 3), centred around 0.7. To explain this experimental observation, we need to consider the free-radical nature of cyclohexane oxidation. In fact, cyclohexane oxidation is a radical-based process[7,18] and our mechanistic study (vide infra) also support this mechanism when AgPd/MgO catalysts are used. In case of a radical process the initiation step is the removal of a H· atom from a C_6H_{12} molecule to form a $C_6H_{11}·$ radical that will further react with oxygen under a diffusion regime. Because in our case (Tables 1-3) we do not initiate the reaction by means of organic radical initiators, it follows that the initiation step has to be carried out by the metals present in the system. Our data clearly shows that AgPd nanoparticles are much more efficient for carrying out this process than solely Ag or Pd alone. This might be due to a better surface/substrate interaction or the nanoalloy being more capable of enabling the C-H abstraction reaction due to a different electron density of the catalyst active sites when the two metals are present. Either way, as AgPd nanoparticles are more active than materials comprising only Ag or Pd, this can be classed as a synergetic effect between the two metals. However, whereas the addition of Pd increases the activity of Ag, the selectivity is essentially unmodified, thus showing that either the single metal or the nanoalloy decompose CHHP in the same manner. For the impregnated catalysts we think that changes in both conversions and selectivity are induced by the probable formation of Ag_2O.[15]**Mechanistic insights and CHHP decomposition**
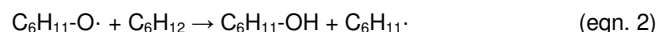
As all our catalysts presented an excess of alcohol with respect to the ketone, and cyclohexane oxidation is known to occur as a free-radical process over Au or Co systems, we were interested in exploring the mechanistic features underlying the observed behaviour for our catalysts. A key intermediate in the oxidation of cyclohexane is cyclohexyl hydroperoxide (CHHP), which can transform to produce cyclohexanone or cyclohexanol.[18,19] Given the importance of CHHP in this reaction, it is necessary to consider the accepted models for the formation of cyclohexanol and cyclohexanone during an autoxidation process mediated by the decomposition of CHHP. This will provide a starting point for considering the catalytic tests using cyclohexyl hydroperoxide, *tert*-butyl hydroperoxide, and the spin trapping experiments, as well as a rationale for the observed selectivity when AgPd/MgO is used.

CHHP can decompose by cleavage of the O-O bond of the hydroperoxide group either *via* thermal decomposition or

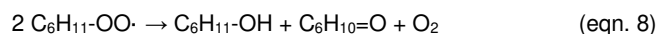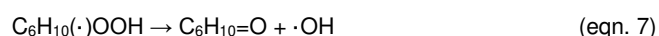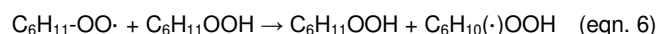assisted by a metal centre.[20] This decomposition leads to the formation of an alkoxy and a hydroxy radical (eq. 1):

$$C_6H_{11}\text{-}OOH \rightarrow C_6H_{11}\text{-}O\cdot + \cdot OH \qquad \text{(eqn. 1)}$$
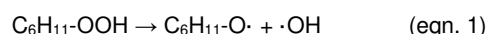
Both of these radicals can react further with cyclohexane to yield to cyclohexanol and a $C_6H_{11}\cdot$ radical (eq. 2), as well as forming water and another $C_6H_{11}\cdot$ radical respectively (eq. 3):

$$C_6H_{11}\text{-}O\cdot + C_6H_{12} \rightarrow C_6H_{11}\text{-}OH + C_6H_{11}\cdot \qquad \text{(eqn. 2)}$$

$$\cdot OH + C_6H_{12} \rightarrow H_2O + C_6H_{11}\cdot \qquad \text{(eqn. 3)}$$

Once the $C_6H_{11}\cdot$ radical is formed, this can quickly react with molecular oxygen, in a diffusion limited reaction step[21] leading to the formation of cyclohexyl peroxide ($C_6H_{11}\text{-}OO\cdot$, abbreviated to CHP) and cyclohexyl hydroperoxide ($C_6H_{11}\text{-}OOH$, CHHP) (eqns. 4 - 5):

$$C_6H_{11}\cdot + O_2 \rightarrow C_6H_{11}\text{-}OO\cdot \qquad \text{(eqn. 4)}$$

$$C_6H_{11}\text{-}OO\cdot + C_6H_{12} \rightarrow C_6H_{11}\text{-}OOH + C_6H_{11}\cdot \qquad \text{(eqn. 5)}$$

The CHP/CHHP molecules can then initiate a series of reactions for the formation of cyclohexanol and cyclohexanone, involving H-α abstraction (eqns. 6-7)[22] and alkyl peroxide disproportionation (the termination reaction given by eqn. 8).[23]

$$C_6H_{11}\text{-}OO\cdot + C_6H_{11}OOH \rightarrow C_6H_{11}OOH + C_6H_{10}(\cdot)OOH \qquad \text{(eqn. 6)}$$

$$C_6H_{10}(\cdot)OOH \rightarrow C_6H_{10}=O + \cdot OH \qquad \text{(eqn. 7)}$$

$$2\ C_6H_{11}\text{-}OO\cdot \rightarrow C_6H_{11}\text{-}OH + C_6H_{10}=O + O_2 \qquad \text{(eqn. 8)}$$

It should be noted that the usual initiation step for the free radical pathway involves the abstraction of a H atom from cyclohexane to from a cyclohexyl radical ($C_6H_{12} \rightarrow C_6H_{11}\cdot$), in a process which can be mediated by the walls of the reactor.[24] In this scheme no alkoxy radical is needed to initiate the reaction, and the ketone (cyclohexanone in our case), will always be formed as a consequence of the autoxidation pathway involving the CHP/CHHP pair (eqns. 6-8). In other words, if a pure radical pathway takes place in solution, the ketone will always form in excess with respect to the alcohol. Current autoxidation models report a K/A ratio of about 1-1.5 if no selectivity control by a catalyst surface is occurring.[25] It follows then that the only way to obtain an excess of alcohol from eqns 1-8 is to have fast cleavage of the O-O bond in CHHP (eqn. 1).[26]

-

In order to identify any trend between the CHHP decomposition and the alcohol formation (Tables 1 and 2) during the oxidation process, the catalysts Pd/MgO, AgPd/MgO and Ag/MgO were tested using CHHP as a substrate (Table 4).

Table 4. Conversion and product distribution in the CHHP decomposition by Pd/MgO, AgPd/MgO and Ag/MgO obtained *via* sol immobilization. Reaction conditions: 1 mL solution 2.5 mol% CHHP in cyclohexane, 6 mg catalysts, 70°C, 0.5 hour. At this temperature no oxidation of cyclohexane occurs, but CHHP decomposition.

Catalyst[a]	Conversion (%)	Selectivity (%)			
		K[b]	A[c]	Total[d]	K/A
Pd/MgO	66	26	74	100	0.35
AgPd/MgO	100	30	70	100	0.43
Ag/MgO	97	24	76	100	0.32

[a] Catalyst prepared by sol immobilization method, for AgPd/MgO a Ag:Pd molar ratio of 1:1 was used. [b] K = ketone, cyclohexanone. [c] A = alcohol, cyclohexanol. [d] Total observed selectivity.

The catalytic decomposition of CHHP to cyclohexanol and cyclohexanone is nearly complete when AgPd/MgO and Ag/MgO are used (*ca.* 100 %), whereas a value of *ca.* 66% conversion was measured in case of Pd/MgO. Therefore the higher the rate of CHHP decomposition, the higher is the activity of the catalysts towards cyclohexane oxidation.

EPR Spin Trapping for the CHHP Decomposition by Ag- Pd- and AgPd/MgO catalysts.

In order to further investigate the correlation between the catalytic activity and the intermediates involved in this reaction (such as alkyl peroxide, alkyl hydroperoxide and alkoxy radicals), we investigated the role of CHHP by using the EPR spin trapping method.[27] The spin-trapping methodology relies on the trapping of short-lived radicals by a diamagnetic spin trap molecule, forming a stable spin adduct,[28] *i.e.* a persistent free radical with a sufficiently long lifetime to enable detection by continuous wave (CW) EPR spectrosocpy. In our case 5,5-dimethyl-1-pyrroline-N-oxide (abbreviated DMPO) was used as the spin trap (Figure 4, top). As a consequence of the different hyperfine couplings between the unpaired electron in the spin adduct and the H in the beta position of DMPO, it is possible to qualitatively evaluate and indirectly identify the nature of the

original short-lived radicals present in solution (through the a_N and a_H coupling constants).[29,30]

It should also be mentioned that a number of intrinsic pressure and temperature limitations are associated with this method of radical detection which collectively prohibit the experiments being conducted at 140°C and 3 bar.[31] As a result, the EPR spin trapping experiments were carried out at room temperature and atmospheric pressure. However, owing to the high sensitivity of the EPR technique, this approach is still sufficient to capture and detect the spin adduct species for analysis.[32]

The X-band CW EPR spectra obtained using the spin trap DMPO during the decomposition of CHHP with Ag-only, Pd-only and AgPd/MgO catalysts in cyclohexane are shown in Figure 3.
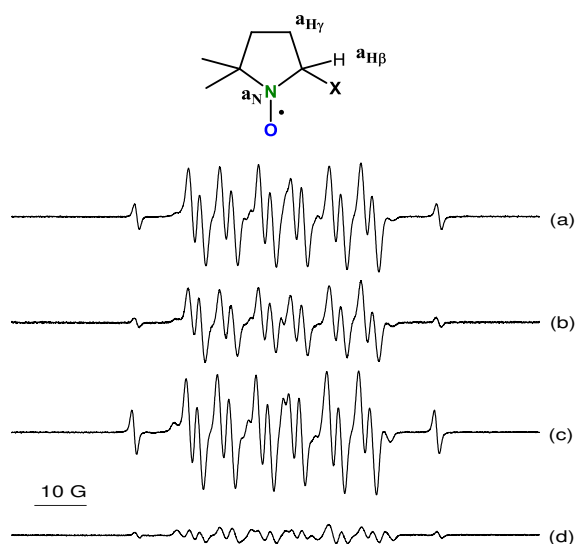

Figure 3. EPR spectra of DMPO spin adducts obtained during the decomposition of CHHP in cyclohexane in the presence of: (a) AgPd/MgO, (b) Pd/MgO, (c) Ag/MgO, and (d) autoxidation with no catalyst. All catalysts were prepared *via* sol immobilization.

A representative EPR spin adduct spectrum, including the combined simulation and deconvoluted single spin adduct species, is reported for the AgPd/MgO catalyst in Figure 4. Simulation of the spectrum and comparison with literature values makes it possible to identify the following species: a di-*tert*-butyl-nitroxide derivative (with $a_N = 14.30$ G),[33] a DMPO–O–C_6H_{11} spin adduct ($a_N = 13.37$, $a_{H(\beta)} = 5.95$, $a_{H(\gamma)} = 1.91$ G),[34] a DMPO–OO–C_6H_{11} adduct ($a_N = 14.46$, $a_H = 10.21$ G),[35] and a carbon-centred adduct possibly originating from a ring opening species tentatively assigned as DMPO–C(OH)R$_2$ ($a_N = 15.93$, $a_H = 21.31$ G)[36] as the catalyst is capable to generate small amounts of adipic acid.
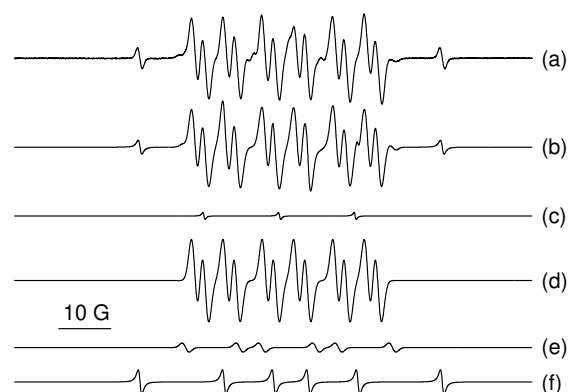

Figure 4. Deconvoluted EPR spectra of DMPO spin adducts obtained during the decomposition of CHHP in cyclohexane in the presence AgPd/MgO with a Ag:Pd molar ratio of 1:1. (a) experimental spectrum and b simulated spectrum, (b) simulated spectrum, (c) di-tert-butyl-nitroxide derivative, (d) DMPO–O–C_6H_{11} spin adduct, (e) DMPO–O_2–C_6H_{11} adduct, and (f) carbon centred adduct, which is possibly a DMPO–C(OH)R$_2$ species.

In order to improve the clarity of our discussion, a schematic illustration of the spin trapping principle, together with structure of the spin adducts we have detected, are reported in Figure 5.
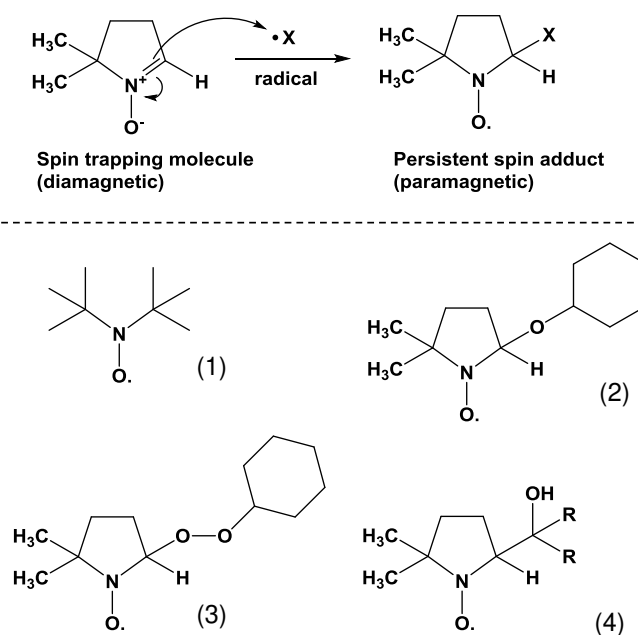

Figure 5. (A) Principle of the spin trapping methodology: fast selective addition (trapping) of short-lived radicals to a diamagnetic spin trap, usually a nitrone or a nitroso compound, such as 5,5-dimethyl-1-pyrroline-N-oxide (DMPO). The product of this addition (spin adduct) is a persistent free radical (nitroxide) with sufficiently long lifetime to enable detection by conventional EPR spectroscopy. (B) Proposed structures of the DMPO spin-adducts detected in the CHHP decomposion in cyclohexane by AgPd/MgO catalyst prepared by sol-immobilization (cross reference with Figure 4): (1) di-tert-butyl-nitroxide derivative, (2) DMPO–O–C_6H_{11} spin adduct, (3) DMPO–O_2–C_6H_{11} adduct, and (4) carbon centred adduct, which is possibly a DMPO–C(OH)R$_2$ species.

6

From the illustration of the spin trapping principle (Figure 5A), it appears that the spin trapping technique only enables one to obtain a semi-quantitative determination of the spin adducts. This is due to the fact that the absolute amount of adduct in solution is the result of several competing factors including the life-time of the spin adduct itself, the nature of the solvent, the temperature and most importantly the efficiency of the trapping reaction in solution by DMPO.[37] However, even after taking these limitations into account, a semi-quantitative analysis can still be conducted since all the catalysts were tested under identical conditions; in other words, any observed differences in the ratios among different spin adducts will be representative of differing catalytic activity.[38] A summary of the relative abundances of spin adducts for CHHP decomposition by Ag-only, Pd-only and AgPd/MgO catalysts is reported in Table 5.

Table 5. Relative abundances (%) of DMPO spin adducts obtained following CHHP decomposition in cyclohexane by Ag-Pd- and AgPd/MgO catalysts.

Catalyst[a]	Nitroxide	RO•	ROO•	C•	Intensity[b]
Pd/MgO	< 0.5%	89	4.6	4.6	183
AgPd/MgO	< 0.5%	90	2.9	6.6	369
Ag/MgO	< 0.5%	89	6.6	4.1	420

[a] Catalyst prepared by sol immobilization method, with a Ag:Pd molar ratio of 1:1. [b] Compared to $5 \cdot 10^{-4}$ M TEMPO solution in cyclohexane, which was used as a standard.
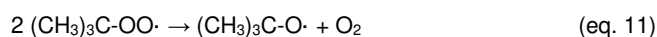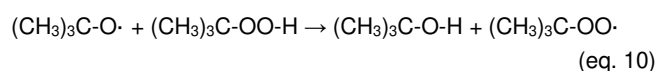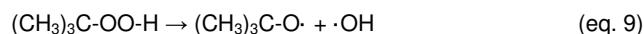
Alkoxy radicals (RO·) are intrinsically more reactive than peroxy radicals (ROO·),[39] and thus an excess of DMPO-OR adducts compared to DMPO-OOR adducts should not be surprising. On the other hand DMPO-O-C_6H_{11} is always present in *ca.* 90% abundance. This means there are no significant variations in the *relative* amounts of this species formed using the different catalysts, and this indicates that large amounts of alkoxy radical are formed in solution, which in turn implies the formation of an excess of alcohol with respect to the ketone. However, whilst the data can explain the observed product distribution for these materials as a whole, it cannot fully explain the higher conversions detected in the presence of Ag/MgO and AgPd/MgO. Since the distribution of the spin adducts is similar for all three catalysts, the total (integrated) area for all of the spin adducts was therefore considered as an estimate for the total amount of intermediates generated during the initial stages of the reaction. The intensity of the experimental EPR spin adduct spectra was compared to a standard solution of TEMPO in cyclohexane (see Table 5, final column).

For Pd/MgO, the least active of the three catalysts, the total number of spins is also the lowest among these three catalysts (Table 5). Therefore, despite the limitation of the semi-quantitative approach to the analysis of the EPR spin trapping data, it is still possible to obtain a correlation between the relative amount of radical intermediates detected and the catalytic activity. It is clear from this analysis that the more active the catalyst is, then a larger amount of radical concentrations are generated in solution (and ultimately trapped by the spin adducts). It is also clear from the EPR results that the three primary adducts detected (RO•, ROO•, C•) can most likely be assigned to the C_6H_{11}-O•, C_6H_{11}-OO• and C_6H_{11}• radicals, and therefore the generic radical based transformation mechanism presented in eqns 1-8 above, is likely to be operative under the current catalytic conditions.

TBHP decomposition

To further extend our mechanistic model beyond the study of CHHP decomposition, we also considered the role and decomposition of *tert*-butyl hydroperoxide (TBHP). TBHP is a common radical initiator,[40] as well as an oxygen donor[41] that can undergo homolytic cleavage of the O-O bond in a similar manner experienced by CHHP (eqs. 9-11).

$$(CH_3)_3C\text{-}OO\text{-}H \rightarrow (CH_3)_3C\text{-}O\cdot + \cdot OH \quad \text{(eq. 9)}$$

$$(CH_3)_3C\text{-}O\cdot + (CH_3)_3C\text{-}OO\text{-}H \rightarrow (CH_3)_3C\text{-}O\text{-}H + (CH_3)_3C\text{-}OO\cdot \quad \text{(eq. 10)}$$

$$2\ (CH_3)_3C\text{-}OO\cdot \rightarrow (CH_3)_3C\text{-}O\cdot + O_2 \quad \text{(eq. 11)}$$

In previous studies, TBHP was identified as an initiator of the free radical processes that enhance the conversion by Au and Pd over Au/MgO[9] and AuPd/MgO[10] supported nanoparticles for the oxidation of cyclohexane. This occurs without altering the K/A ratio of the reaction mixture, but instead by increasing the formation of undesired adipic acid. Thus we were interested in the role played by TBHP in the presence of Ag as relevant to the current study.

Catalytic tests for the cyclohexane oxidation using Ag/MgO and AgPd/MgO catalysts were carried out by using TBHP in small amounts only (0.15 mol % with respect to cyclohexane), to restrict the use of this species to an initiator. TBHP increased the conversion towards cyclohexane oxidation for all the catalysts (Table 6), although selectivity to the alcohol is lost with K/A ratios in the range 0.8-1.0 and results in the formation of

large amounts of adipic acid. This shows similarities with Au and Pd on MgO which give a similar product distribution.[10] On the other hand, these data (compared to Table 3) also show that if AgPd/MgO is used without any organic initiator, the nanoalloy is as good as organic radicals at initiating the reaction, while still minimizing by-product formation. Therefore reaction does not necessarily need to be 'activated' by the presence of an organic radical.

Table 6. Catalytic performance of metallic catalysts in presence of TBHP initiator (TBHP to cyclohexane 0.15 % molar ratio). Reaction conditions: Pressure = 3 bar, temperature =140°C, reaction time = 17 h.

Catalyst	Conversion (%)	Selectivity (%)				
		K[c]	A[d]	CHHP[e]	AA[f]	Total[g]
Ag_1Pd_1/MgO[a]	12	32	36	0	32	100
Ag/MgO [a]	9	28	37	0	30	95
Ag/MgO[b]	6.3	32	52	0	11	95
TBHP	6.6	33	52	0	15	100

[a] Catalyst prepared by sol immobilization method. [b] Catalyst prepared by impregnation method. [c] K = ketone, cyclohexanone. [d] A = alcohol, cyclohexanol. [e] CHHP = cyclohexyl hydroperoxide. [f] AA = adipic acid. [g] Total observed selectivity.

In this context though, there is no apparent difference between the blank test in the presence of just TBHP and the test using a Ag/MgO catalyst prepared by impregnation on MgO. We believe this is due to the presence of Ag_2O in this particular catalyst. As TBHP exerts its initiator activity as a consequence of the cleavage of its O-O bond, this would suggest that sol-immobilized AgPd/mgO catalysts (that are richer in Ag^0) are more efficient at carrying out this particular reaction.

Conclusions

We have shown that silver nanoparticles can be an efficient catalyst for the oxidation of cyclohexane, with enhanced selectivity towards cyclohexanol and a limited formation of adipic acid, and thus are a viable catalytic system for this important oxidation reaction. The activity of the silver nanoparticles was found to be highly dependent on the preparation method used to deposit them onto MgO. The supported nanoparticles were most active if a sol-immobilization method was used to prepare the catalyst, whereas a diminished catalytic activity along with a change in the product distribution was found if the catalysts were prepared by an impregnation method. This result is tentatively ascribed to the presence of Ag_2O species for the impregnated catalysts, and the presence of reduced Ag metal for the sol-immobilized nanoparticles. The effect of a second metal such as Pd, to induce the formation of nanoalloys with Ag, led to a synergistic effect towards cyclohexane oxidation. In particular,

Ag-Pd/MgO catalysts had higher conversion compared to the Ag monometallic catalysts, but without losing the high selectivity to cyclohexanol or without generating large amounts of adipic acid, and thus showing great potential for the exploitation of silver nanoalloys in this area. An optimal Ag-Pd composition of these materials, for enhanced conversion, was identified to be an equimolar amount of the two metals. Furthermore, characterization of the catalysts presenting the same nominal metal loading for Ag and Pd revealed a wide nanoparticle size range (from *ca.* 2 nm to about 40 nm) with small particles that are proportionally richer in Pd, and larger nanoparticles that are richer in Ag.

Finally, the mechanistic aspects of the catalytic transformation were investigated using the EPR spin trapping technique, which showed that AgPd/MgO and Ag/MgO catalysts prepared by sol immobilization were more active compared to the Pd/MgO catalyst, as they were capable of forming a higher concentration of the CHHP species, and in turn alkoxy radicals in solution and from this high cylohexanol selectivity is possible.

Experimental Section

Chemicals

$AgNO_3$, $PdCl_2$, MgO, cyclohexane and other chemicals were purchased from Aldrich and used without further purification unless otherwise specified.

Catalyst preparation

Ag-Pd/MgO catalysts (1 wt% total metal loading) were prepared by using a modified sol-immobilisation method as reported in [42] and the references therein. The desired amount of $AgNO_3$ (Sigma Aldrich, assay 99% wt) and $PdCl_2$ (Sigma Aldrich, assay 99% wt) were added into 800 mL water. After stirring for 15 min, 1.3 mL of PVA solution (0.01 g mL^{-1}) was added, and the solution was stirred for a further 15 mins. Subsequently, 3.3 mL of freshly prepared $NaBH_4$ solution (0.1 M) was added to generate Ag-Pd nanoalloy particles. After reduction for 45 min, the MgO support (Sigma Aldrich, 1.98 g) was added to immobilise the nanoparticles. After filtration and washing, the solid obtained was dried (110 ºC, 16 h) before use. The relative amount of Ag and Pd salts used was varied to obtain a systematic series of supported catalysts with different molar ratios of Ag to Pd, ranging from 10:1 to 1:10. It is well established that the use of PVA as a colloid stabiliser prevents their sintering before their immobilization on a support.[43] As the surfactant can be easily removed at about 100 ºC, we consider the activity of these catalysts are not significantly affected by the presence of residual PVA on the metal or the support. Mono-metallic Ag and Pd supported catalysts, were also prepared for comparative purposes using the same total metal loading (*i.e.* 1 wt%). An additional Ag/MgO catalyst (1 wt%) was also prepared using impregnation method for comparative purposes. For this catalyst, the desired amount of $AgNO_3$ was added into 20 mL water containing a suspension of MgO. The resulting slurry was dried at (110 ºC, 16 h), and the catalyst was reduced using H_2 (5% in Ar) at 400 °C for 30 min.

Catalytic tests and characterization of the products

Oxidation of cyclohexane (Alfa Aesar, 8.5 g, HPLC grade) was carried out in a glass bench reactor using a fixed mass of catalysts (6 mg) for all tests. The reaction mixture was magnetically stirred at 140 °C and 3 bar O_2 for 17 h. Samples of the reaction mixture were analysed by gas chromatography, using a Varian 3200 GC equipped with a flame ionization detector. Chromatographic separation and identification of the products was carried out using a CP-Wax 42 column. Adipic acid present in the reaction mixture was converted to its corresponding ester for quantification purposes, and chlorobenzene was added as an internal standard. The product distribution as a function of reaction time was monitored by studying a systematic series of reaction batches subjected to different reaction times under the same conditions of temperature and oxygen partial pressure. The experimental error associated to our methods though does not allow us to statistically discriminate conversion values less than or equal to *ca.* 1%, . Measured conversion levels in this range should therefore be considered as statistically identical.

Re-usability tests

Re-usability tests were also performed in an identical glass reactor. Cyclohexane (8.5 g) and an excess of 1 wt% Ag-Pd/MgO (60 mg) were added into the batch reaction and catalytic oxidation was carried out at 140 °C and 3 bar O_2 for 17 h. After reaction, the used catalyst was washed with cyclohexane and dried at 110oC for 16 h. Afterwards, the catalytic activity of the used Ag-Pd/MgO catalyst was tested under same reaction conditions: Ag-Pd/MgO (total metal loading 1 wt%, 6 mg), cyclohexane (8.5 g), at 140 °C and 3 bar O_2 for 17 h). The obtained reaction mixture was analysed by gas chromatography as described in the catalytic tests and characterization of the products paragraph. Subsequent re-usability tests were carried out on the same material following same procedure.

CHHP and TBHP decomposition

Cyclohexyl hydroperoxide (CHHP), was synthesized by a Grignard reagent-oxygen reaction, as reported in [44] and the references therein. A solution containing 2.5 mol% cyclohexyl hydroperoxide in cyclohexane was obtained. Catalytic decomposition of CHHP was carried out in V-Vials with total volume of 3 mL. The CHHP solution (1 mL) was mixed with the catalyst (6 mg) under continuous stirring conditions at 70°C for 30 min. After reaction, the solution was immediately cooled using an ice-water bath. The sample was centrifuged and the liquid analysed by GC.
The influence of the radical initiator, *tert*-butyl hydroperoxide (TBHP) (Sigma Aldrich, 70 wt% in water) was also studied in this work. Cyclohexane (8.5 g) and TBHP (20 mg) were added into the glass reactor with or without catalysts, and then catalytic oxidation was conducted under the same reaction conditions (140 °C, 3 bar O_2, 17 hours, 6 mg catalysts). The products were analysed by the GC following the procedure as described in the catalytic tests and characterization of the products section.

EPR experiments

X-band continuous wave (CW) EPR spectra were recorded at room temperature in deoxygenated cyclohexane, using a Bruker EMX spectrometer equipped with a high sensitivity Bruker ER 4119 cavity. The typical instrument parameters were: centre field 3487 G, sweep width 100 G, sweep time 55 s, time constant 10 ms, microwave power 5 mW, modulation frequency 100 kHz, and modulation width 1 G. Spectral analysis was carried out using the WinSim software.[45] The spin trapping experiments were performed using the following procedure: 5,5-dimethyl-1-pyrroline N-oxide (DMPO) (0.1 mL of 0.1 M solution in cyclohexane) was added to the substrate (0.1 mL of 2.5 mol% solution of CHHP in cyclohexane) in an EPR sample tube. The mixture was deoxygenated by bubbling N2 through the solution for 1 min prior to recording the EPR spectrum in order to enhance the signal resolution.[46] For the reactions involving the Ag/MgO, Pd/MgO and Ag-Pd/MgO catalysts, deoxygenation was carried out at room temperature 5 min after the mixing of the catalyst with the reaction mixture.

Electron Microscopy Characterisation

Samples of catalysts were prepared for TEM/STEM analysis by dry dispersing the catalyst powder onto a holey carbon TEM grid. Bright field (BF) imaging experiments were carried out on a JEOL 2000FX TEM operating at 200 kV. High-angle annular dark field (HAADF) imaging experiments were carried out using a 200 kV JEOL 2200FS scanning transmission electron microscope equipped with a CEOS aberration corrector. This latter microscope was also equipped with a Thermo-Noran X-ray energy dispersive spectroscopy (XEDS) system for compositional analysis.

[1] M. Eichelbaum, R. Glaum, M. Hvecker, K. Wittich, C. Heine, H. Schwarz, C.-K. Dobner, C. Welker-Nieuwoudt, A. Trunschke, R. Schlögl, *ChemCatChem* **2013**, *5*, 2318–2329.

[2] U. Schuchardt, D. Cardoso, R. Sercheli, R. Pereira, R. S. da Cruz, M. C. Guerreiro, D. Mandelli, E. V. Spinacé, E. L. Pires, *Appl. Catal. A: Gen.* **2001**, *211*, 1–17.

[3] C. Hess, M. H. Looi, S. B. A. Hamid, R. Schlögl, *Chem. Commun.* **2006**, 451–453.

[4] R. Y. Saleh, I. E. Wachs, S. S. Chan, C. C. Chersich, *J. Catal.* **1986**, *98*, 102–114

[5] Y. Ishii, S. Sakaguchi, T. Iwahama, *Adv. Synth. Catal.* **2001**, *343*, 393–427.

[6] J.-M. Brégeault, *Dalton Trans.* **2003**, 3289–3302.

[7] X. Liu, Y. Ryabenkova, M. Conte, *Phys. Chem. Chem. Phys.* **2015**, *17*, 715-731.

[8] W. Yao, Y. Chen, L. Min, H. Fang, Z. Yan, H. Wang, J. Wang, *J. Mol. Catal. A: Chem.* **2006**, *246*, 162–166.

[9] C.-C. Guo, M.-F. Chu, Q. Liu, Y. Liu, D.-C. Guo, X.-Q. Liu, *Appl. Catal. A: Gen.* **2003**, *246*, 303–309.

[10]   X. Liu, M. Conte, M. Sankar, Q. He, D. M. Murphy, D. Morgan, R. L. Jenkins, D. Knight, K. Whiston, C. J. Kiely, G. J. Hutchings, *Appl. Catal. A: Gen.* **2015**, *504*, 373–380.

[11]   M. Conte, X. Liu, D. M. Murphy, K. Whiston, G. J. Hutchings, *Phys. Chem. Chem. Phys.* **2012**, *14*, 16279–16285.

[12]   Y. Lei, F. Mehmood, S. Lee, J. Greeley, B. Lee, S. Seifert, R. E. Winans, J. W. Elam, R. J. Meyer, P. C. Redfern, D. Teschner, R. Schlögl, M. J. Pellin, L. A. Curtiss, S. Vajda, *Science* **2010**, *328*, 224–228.

[13]   N. Dimitratos, L. Prati, *Gold Bull.* **2005**, *38*, 73–77.

[14]   U. Schuchardt, W. A. Carvalho, R. Pereira, E. V. Spinacé in: Cyclohexane Oxidation: Can Gif Chemistry Substitute for the Classical Process? (The Activation of Dioxygen and Homogeneous Catalytic Oxidation, Eds.: D. H. R. Barton, A. E. Martell, D. T. Sawyer, Springer US, New York, **1993**, pp. 243–255.

[15]   M. Conte, J. A. Lopez-Sanchez, Q. He, D. J. Morgan, Y. Ryabenkova, J. K. Bartley, A. F. Carley, S. H. Taylor, C. J. Kiely, K. Khalid, G.J. Hutchings, *Catal. Sci. Technol.* **2012**, *2*, 105–112.

[16]   A. Villa, D. Wang, G. M. Veith, F. Vindigni, L. Prati, *Catal. Sci. Technol.* **2013**, *3*, 3036–3041.

[17]   H. N. Vasan, C. N. R. Rao, *J. Mater. Chem.* **1995**, *5*, 1755–1757.

[18]   I. Hermans, P. A. Jacobs, J. Peeters, *Chem. Eur. J.* **2007**, *13*, 754–761.

[19]   B. P. C. Hereijgers, B. M. Weckhuysen, *J. Catal.* **2010**, *270*, 16–25.

[20]   I. A. Salem, M. El Maazawi, A. B. Zaki, *Int. J. Chem. Kinet.* **2000**, *32*, 643–666.

[21]   M. S. Stark, *J. Am. Chem. Soc.* **2000**, *122*, 4162–4170.

[22]   I. Hermans, J. Peeters, P. Jacobs, *ChemPhysChem* **2006**, *7*, 1142–1148.

[23]   W. Partenheimer, *Catal. Today* **1995**, *23*, 69–158.

[24]   M. Conte, H. Miyamura, S. Kobayashi, V. Chechik, *Chem. Commun.* **2010**, *46*, 145–147.

[25]   I. Hermans, P. A. Jacobs, J. Peeters, *Chem. Eur. J.* **2006**, *12*, 4229–4240.

[26]   J.-R. Chen, H.-H. Yang, C.-H. Wu, *Org. Process Res. Dev.* **2004**, *8*, 252–255.

[27]   C. M. Jones, M. J. Burkitt, *J. Am. Chem. Soc.* **2003**, *125*, 6946–6954.

[28]   M. Conte, K. Wilson, V. Chechik, *Org. Biomol. Chem.* **2007**, *7*, 1361–1367.

[29]   M. Conte, K. Wilson, V. Chechik, *Org. Biomol. Chem.* **2007**, *7*, 1361–1367.

[30]   D. R. Duling, *J. Magn. Reson. B* **1994**, *104*, 105–110.

[31]   M. Conte, K. Wilson, V. Chechik, *Rev. Sci. Instrum.* **2010**, *81*, 104102.

[32]   M. Conte, X Liu, D. M. Murphy, S. H. Taylor, K. Whiston, G. J. Hutchings, *Catal. Lett.* **2016**, *146*, 126–135.

[33]   M. Novak, B. A. Brodeur, *J. Org. Chem.* **1984**, *49*, 1142–1144.

[34]   S. L. Baum, I. G. M. Anderson, R. R. Baker, D. M. Murphy, C. C. Rowlands, *Anal. Chim. Acta* **2003**, *481*, 1–13.

[35]   M. J. Davies, T. F. Slater, *Biochem. J.* **1986**, *240*, 789–795.

[36]   E. G. Janzen, C. A. Evans, J. P. Liu, *J. Magn. Reson.* **1973**, *9*, 513–516.

[37]   P. Ionita, M. Conte, B. C. Gilbert, V. Chechik, *Org. Biomol. Chem.* **2007**, *5*, 3504–3509.

[38]   M. Conte, H. Miyamura, S. Kobayashi, V. Chechik, *J. Am. Chem. Soc.* **2009**, *131*, 7189–7196.

[39]   B. W. Griffin, *Can. J. Chem.* **1982**, *60*, 1463–1473.

[40]   R. Raja, G. Sankar, J. M. Thomas, *J. Am. Chem. Soc.* **1999**, *121*, 11926–11927.

[41]   W. Adam, B. Nestler, *J. Am. Chem. Soc.* **1993**, *115*, 7226–7231.

[42]   J. A. Lopez-Sanchez, N. Dimitratos, P. Miedziak, E. Ntainjua, J. K. Edwards, D. Morgan, A. F. Carley, R. Tiruvalam, C. J. Kiely, G. J. Hutchings, *Phys. Chem. Chem. Phys.* **2008**, *10*, 1921–1930.

[43]   J. A. Lopez-Sanchez, N. Dimitratos, C. Hammond, G. L. Brett, L. Kesavan, S. White, P. Miedziak, R. Tiruvalam, R. L. Jenkins, A. F. Carley, D. Knight, C. J. Kiely, G. J. Hutchings, *Nat. Chem.* **2011**, *3*, 551-556.

[44]   C. Walling, S. A. Buckler*, J. Am. Chem. Soc.* **1955,** 77, 6032–6038.

[45]   Simulations were carried out using WinSim software: http://www.niehs.nih.gov/research/resources/software/tox-pharm/tools/index.cfm

[46]   M. Conte, Y. Ma, C. Loyns, P. Price, D. Rippon, V. Chechik, *Org. Biomol. Chem.* **2009**, *7*, 2685–2687.